Development of an ineffective pea root nodule: morphogenesis, fine structure, and cytokinin biosynthesis

WILLIAM NEWCOMB,[1] KUNIHIKO SYŌNO,[2] AND JOHN G. TORREY[3]

Department of Botany and Genetics, University of Guelph, Guelph, Ont., Canada, N1G 2W1, and Cabot Foundation, Harvard University, Petersham, MA, U.S.A. 01366

Received December 1, 1976

NEWCOMB, W., K. SYŌNO, and J. G. TORREY. 1977. Development of an ineffective pea root nodule: morphogenesis, fine structure, and cytokinin biosynthesis. Can. J. Bot. **55**: 1891–1907.

Roots of the garden pea *Pisum sativum* L. cv. Little Marvel inoculated with *Rhizobium leguminosarum* strain 1019 produce small white nodules which are ineffective in fixing atmospheric nitrogen. Analyses of cytokinin contents of the nodules at different ages using extraction, purification, and thin-layer chromatographic separation showed that the cytokinins zeatin and zeatin riboside and isopentenyladenine and its riboside were present in greatest amounts early in nodule development and decreased thereafter. A new unidentified cytokinin was present in older nodules. The early stages of the infection process in the ineffective nodules were similar to those observed in effective nodules. However, bacteria released from the bacterial thread via an unwalled droplet were not always surrounded by a host membrane. In later stages of nodule development many infected cells contained rhizobia with no enclosing membranes so that the bacteria were free within the host cytoplasm. Such cells showed very low frequencies of mitochondria, of polyribosomes, and endoplasmic reticulum. Thus, the biosynthetic capacity of the cells appeared to be impaired and membrane synthesis defective. The failure of the nodules to develop nitrogenase activity is probably related to the failure of membrane formation around the bacteria. Abnormalities in amyloplast formation were also noted, as well as structural differences in the nodule, including a higher proportion of uninfected cells and earlier cessation of mitotic activity in the nodule meristem than occurs in effective nodules of pea. Transfer cells were observed in the pericycle in both effective and ineffective nodules.

NEWCOMB, W., K. SYŌNO et J. G. TORREY. 1977. Development of an ineffective pea root nodule: morphogenesis, fine structure, and cytokinin biosynthesis. Can. J. Bot. **55**: 1891–1907.

L'inoculation de plants de pois, *Pisum sativum* L. cv. Little Marvel inoculés avec la souche 1019 du *Rhizobium leguminosarum* produit de petits nodules blancs inefficaces à fixer l'azote atmosphérique. Des analyses de contenus en cytokinines à différents âges, conduites par extraction, purification et séparation chromatographique sur couche mince, montrent que les cytokinines telles que la zéatine, la zéatine riboside ainsi que l'isopenténylad énine et ses ribosides se retrouvent en quantités plus forte au début de la formation du nodule et diminuent par la suite. Une nouvelle cytokinine non-identifiée existe chez les nodules plus âgés. Les premières étapes du processus d'infection dans la formation des nodules inefficaces sont semblables à celles qu'on peut observer chez les nodules efficaces. Cependant, les bactéries libérées du cordon d'infection dans une gouttelette sans paroi ne sont pas toujours entourées par la plasmalemme de l'hôte. Aux étapes plus avancées du développement, plusieurs cellules infectées contiennent des rhizobiums sans enveloppe membranaire de sorte que les bactéries sont nues dans le cytoplasme de l'hôte. De telles cellules montrent une faible abondance de mitochondries, de ribosomes et de réticulum endoplasmique. Ainsi, la capacité biosynthétique des cellules semble déréglée et la synthèse membranaire déficiente. L'incapacité des nodules à développer une activité nitrogénasique est probablement reliée à l'échec de la formation d'une membrane autour des bactéries. Les auteurs ont également noté des anomalies dans la formation des amyloplastes ainsi que des différences structurales dans le nodule incluant une plus forte proportion de cellules non-infectées et un arrêt plus hâtif de l'activité mitotique dans le méristème du nodule que ce qu'on observe dans les nodules efficaces du pois. Des cellules de transfert existent dans le péricycle des nodules inefficaces aussi bien qu'efficaces.

[Traduit par le journal]

Introduction

The establishment of the capacity for symbiotic nitrogen fixation in leguminous species involves the interaction of the host and endophyte genomes resulting in a complex sequence of developmental changes and morphogenetic

[1]Present address: Department of Botany and Genetics, University of Guelph, Guelph, Ont., Canada N1G 2W1.

[2]Present address: Department of Pure and Applied Sciences, University of Tokyo, 3-8-1 Komaba, Meguro-ku, Tokyo 153, Japan.

[3]Present address: Cabot Foundation, Harvard University, Petersham, MA, U.S.A. 01366.

events during the initiation, growth, differentiation, and senescence of the root nodule (Dart 1974, 1975; Newcomb 1976). Mutations in the host and (or) *Rhizobium* genome as well as adverse environmental conditions may result in the formation of ineffective root nodules that do not fix molecular nitrogen (Bergersen 1957, 1974; Nutman 1969; Dart 1974, 1975; Brill 1974; Holl 1975). Ineffective nodules may differ from effective nodules of the same species or cultivar in both their physiology and structure (Pankhurst 1974) or they may be similar in structure to effective nodules but not fix molecular nitrogen (Holl 1973; Bergersen 1974).

Rhizobium leguminosarum strain 1019 produces small, round, white nodules (on the lateral roots of the garden pea) which become green with age. As cytokinins are present in effective pea nodules (Syōno and Torrey 1976) and are associated with the mitotic activity of the nodule meristem (Syōno *et al.* 1976), the development of the ineffective nodules was studied to determine the influence of cytokinins on the morphogenesis of these abnormal organs. This report describes cytokinin biosynthesis in relation to the development and fine structure of the ineffective nodules and compares their ontogeny and physiology with those of effective nodules produced on the same cultivar of garden pea.

Materials and Methods

Plant Material

Untreated seeds of the garden pea *Pisum sativum* cv. Little Marvel were soaked in distilled water for 8 h, germinated in washed sand, and on the 5th day placed in aeroponic culture tanks (Zobel *et al.* 1976). On the 6th day the tanks were inoculated with a pure culture of *Rhizobium leguminosarum* strain 1019. Aeroponic culture permitted easy observation of the growing roots and attached nodules which were bathed continuously in a mist of 1/8-strength Hoagland's solution minus nitrogen.

Estimation of Cytokinin Content and Growth Measurements

Nodules were sampled at 12, 18, and 24 days after inoculation and placed in absolute alcohol that had been precooled with dry ice – acetone or in a freezer (−19°C). The cytokinins were then extracted with 80% ethanol. After removal of the ethanol and acidifying to pH 3.0, the aqueous phase was extracted repeatedly with methylene chloride, the pH was adjusted to 8.0, and the aqueous phase was then extracted with 1-butanol. The butanol fraction was concentrated and applied to silica gel GF_{254} plates for thin-layer chromatography and developed with chloroform–methanol (4:1, v/v). Zones were extracted with methanol from the developed plates and cytokinin activity was detected by the soybean callus bioassay. More complete descriptions of the culture methods and conditions for the plants, inoculation of *Rhizobium*, and the techniques of cytokinin extraction, fractionation, chromatography, and bioassay may be found in an earlier paper (Syōno and Torrey 1976). Similarly the procedures used in obtaining the mitotic indices and growth measurements are described in detail elsewhere (Syōno *et al.* 1976).

Tissue Preparation for Microscopy

Median slices of 15-day-old nodules were fixed in 2.5% glutaraldehyde in 0.025 *M* potassium phosphate buffer, pH 6.8, at room temperature for 12 h, rinsed several times in the same buffer at 4°C, postfixed in 1% osmium tetroxide in buffer overnight, dehydrated slowly in methyl cellosolve, ethanol, and propylene oxide, and finally embedded in Araldite (Newcomb 1976). Monitor sections for light microscopy were cut with glass knives at 0.5–1.5 μm, mounted on glass slides, and stained over an alcohol lamp with 0.05% toluidine blue O in 1% sodium tetraborate (borax) buffer. Silver-coloured sections for electron microscopy were also cut with glass knives, stained for 30 min with a saturated solution of uranyl acetate in 50% ethanol before about 7 min in 0.02% lead citrate (Venable and Coggeshall 1965), and examined with either a Philips 200 or a Zeiss EM7 electron microscope.

Observations and Results

Nodule Morphogenesis and Growth

The first macroscopically detectable nodules were white spheres which occurred 10 days after inoculation (Fig. 1). From the 12th to the 24th day the roots increased in average weight per plant. Flower development was apparent by day 18 and fruit development increased rapidly beginning at the 24th day (Fig. 1). Between 12 and 18 days after inoculation, nodule growth proceeded at a rapid rate and subsequently declined (Figs. 1, 2, and 3). The average diameter of ineffective nodules increased about 30% between 12 and 18 days but only about 10% between 18 and 24 days (Fig. 2). Similarly nodule fresh weight and height exhibited a marked increase between 12 and 18 days before a much smaller increase between 18 and 24 days (Figs. 2 and 3). In addition, the average number of nodules per plant increased markedly from 12.6 to 22.6 between 12 and 18 days but showed no increase thereafter (Fig. 3). Because nodule size and growth are largely dependent on the mitotic activity of the nodule meristem from which most of the nodule cells are derived, mitotic indices were determined for nodules of various diameters at three sampling times. Stages of nodule size were established as had been done earlier for normal nodules (Syōno *et al.* 1976). The mitotic index of these ineffective nodules was highest in 12-day-old nodules of stage II and

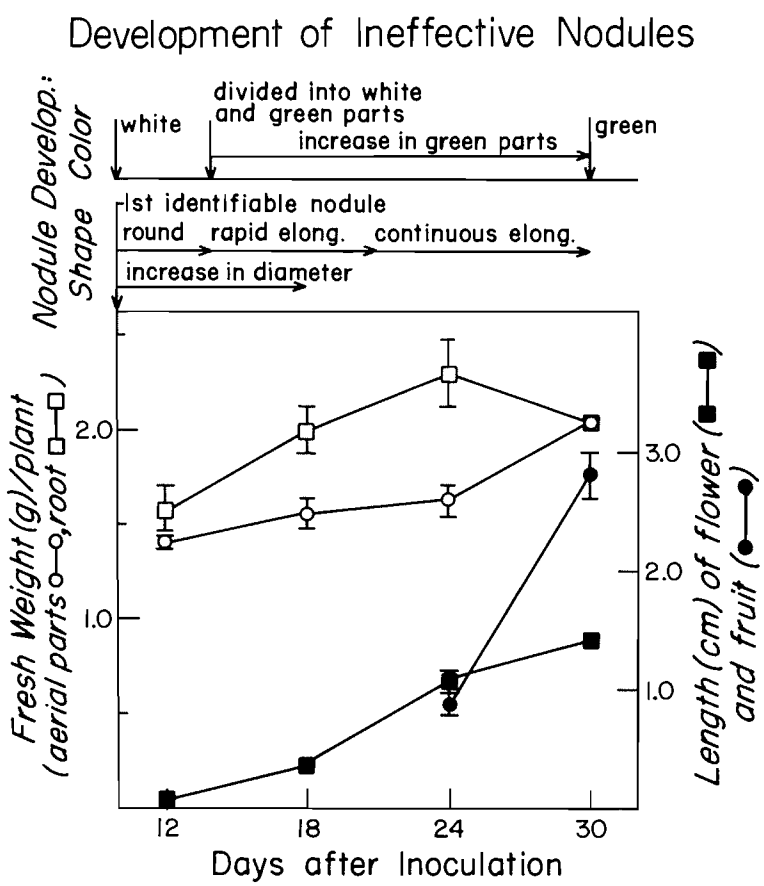

ABBREVIATIONS USED IN THE FIGURES: A, amyloplast; CW, cell wall; G, Golgi body; IC, infected cell; IS, intercellular space; IT, infection thread; M, mitochondrion; N, nucleus; NC, nodule cortex; NM, nodule meristem; Nu, nucleolus; P, proplastid; PBS, peribacteroidal space; PC, pericycle cell; R, rhizobium; RER, rough endoplasmic reticulum; S, starch granule; ST, stele; TM, thread matrix; UC, uninfected cell; UD, unwalled droplet; V, vacuole; WI, wall ingrowth; X, xylem.

FIG. 1. The relationship between nodule development and plant growth at various times after inoculation with *R. leguminosarum* strain 1019. The diagram illustrates nodule colour, shape, and size at various sampling times after inoculation. Average shoot fresh weight (○), root fresh weight (□), flower length (■), and fruit length (●) are compared at various sampling times. Elong., elongation; Develop., development.

declined with increased age (Fig. 4). As had been observed in normal nodules, mitotic activity is related to nodule size. Nodules of stage II had the highest mitotic index at all ages but nodules having smaller or larger diameters exhibited lower mitotic indices (Fig. 4), having not yet reached or already passed the time of maximum mitotic activity.

Cytokinin Production

Cytokinin content was highest in 12-day-old nodules and declined sharply thereafter, such that 18-day-old nodules contained about half that amount; only very low amounts were detected in 24-day-old nodules (Fig. 2). The major cytokinins in 12- and 18-day-old nodules based on cochromatography on thin-layer chromatographic separations were zeatin and its riboside, while in 24-day-old nodules a different and unidentified cytokinin was present (Fig. 5) in addition to much lower levels of zeatin and its riboside. To confirm this interesting result a more concentrated extract from 24-day-old nodules was prepared, rechromatographed, and tested for cytokinin activity in the soybean callus bioassay. The presence of the additional unidentified cytokinin was confirmed along with the presence of low levels of isopentenyladenine

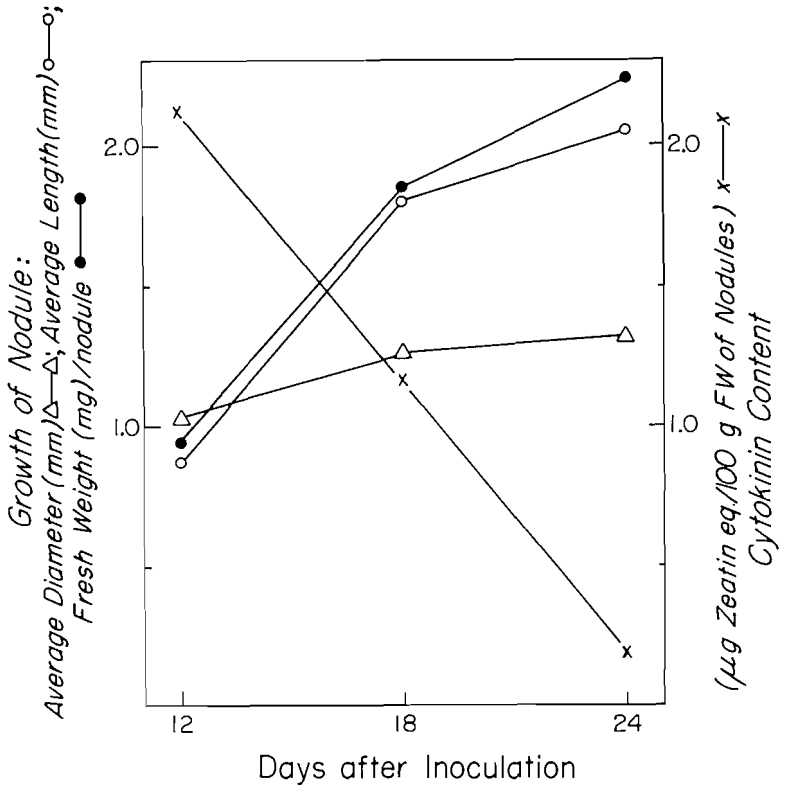

FIG. 2. Graph illustrating the relationship between nodule growth (△), expressed as diameter, length (○), and fresh weight (●), and cytokinin contents (×) (μg zeatin e.g. /100 g fresh weight of nodules) between 12 and 24 days after inoculation. FW, fresh weight; eq., equivalent.

(2iP), isopentenyladenosine (IPA), and zeatin (Z) and its riboside (ZR) (Fig. 6).

Nodule Anatomy

Ineffective pea nodules contain a central zone of tissue surrounded by the nodule cortex, which is comprised of several layers of large vacuolate cells (Fig. 7). The nodule meristem from which most of the nodule cells are derived is located at the distal end of the central mass of nodule tissue. The central region of nodule tissue consists of numerous vacuolate, uninfected cells and fewer numbers of infected cells. The formation of large numbers of amyloplasts both in infected and uninfected cells is apparent. In contrast with the orderly arrangement of developmental stages of infected cells in effective pea nodules (Fig. 1 in Newcomb (1976) and Fig. 1 in Syōno *et al.* (1976)), the various developmental stages of infected cells are arranged more at random in these ineffective pea nodules (Fig. 7). However, in general, the oldest infected cells are nearest the lateral root to which the nodule is attached but often newly infected cells are located adjacent to older or senescing infected cells.

Cytology and Fine Structure

Infection and Bacterial Release

While the infected cells of ineffective pea nodules are less numerous and often differ cytologically from those of effective pea nodules, the infection process in the developing nodule is basically similar in both. Both intracellular and intercellular infection threads are present (Figs. 8 and 9); uninfected cells are invaded and rhizobia are eventually released from the infection thread. Invaginations of the host cell wall give rise to the intracellular infection thread from which bacteria are released at the unwalled regions of the thread or from droplets of thread matrix (Figs. 8–10). The host plasma membrane separates the pea cytoplasm from the infection thread cell wall and also forms the boundary

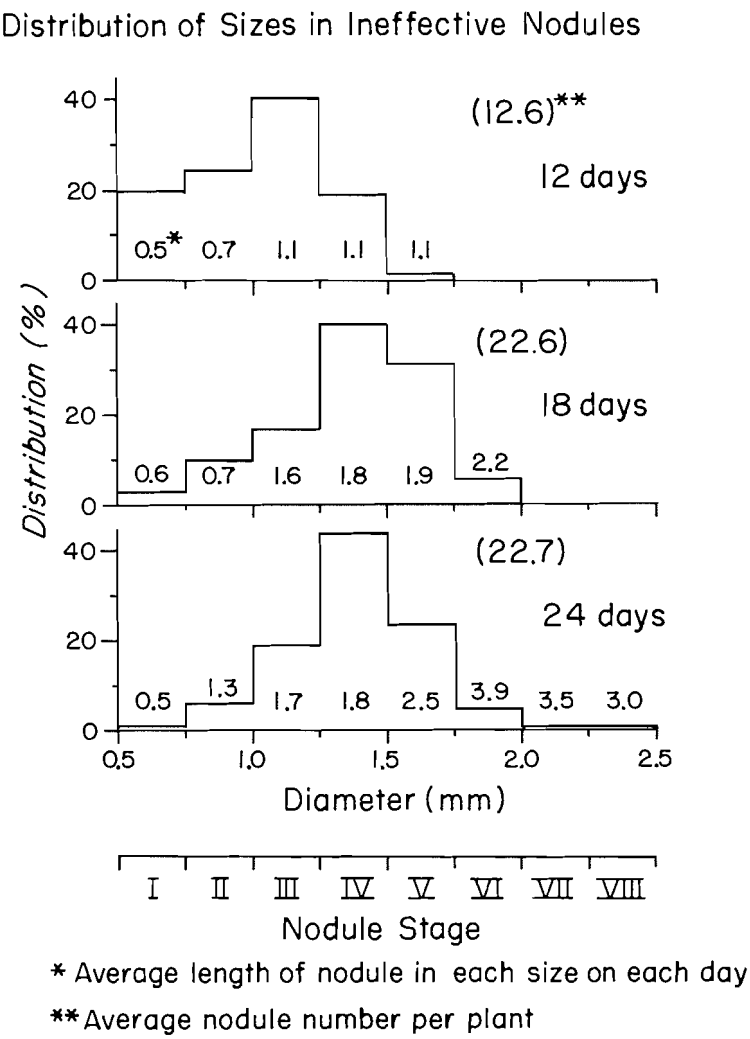

FIG. 3. Distribution or percentage of nodules according to nodule diameter (stage) at 12, 18, and 24 days after inoculation. The average length of nodule in each size class on each day (*) and the average number of nodules per plant (**) are also indicated.

between the host cytoplasm and the unwalled regions of thread and unwalled droplets (Figs. 16–19). The rhizobia are often closely packed within the infection threads and unwalled droplets (Figs. 10 and 19). Within the infection threads and unwalled droplets the bacteria often appear dense and irregularly shaped (Figs. 17 and 18), possibly suggestive of degenerating cells; some rhizobia are less electron dense and contain many ribosomes (Fig. 19), appearing similar to the vegetative bacteria of effective pea nodules.

The release of bacteria occurs from the unwalled regions of the infection thread or unwalled droplets of thread matrix (Figs. 8–10). The rhizobia become closely associated with or possibly attach to the bounding plasmalemma and by endocytosis enter the host cytoplasm (Figs. 16–19). The newly released bacteria are usually surrounded by a membrane envelope derived from the host-cell plasmalemma which bounds the unwalled regions of the thread and unwalled droplets (Figs. 16–19). Occasionally rhizobia which are not completely surrounded by a membrane envelope are released from an unwalled droplet (Figs. 16 and 18), an event never

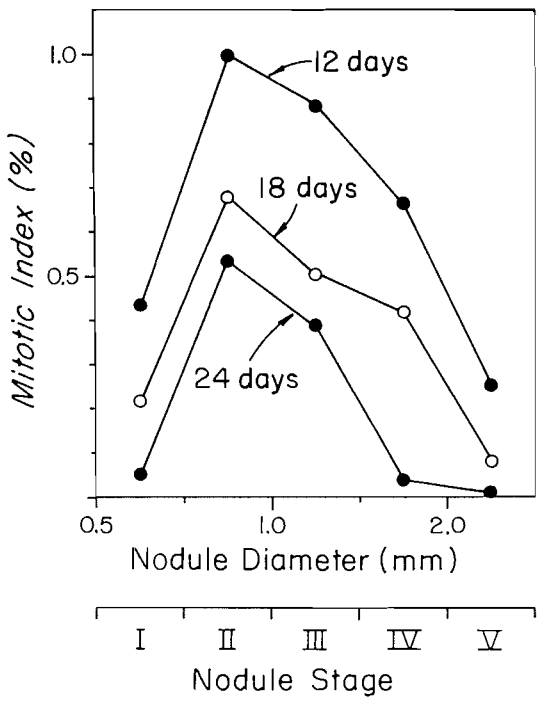

FIG. 4. The relationship between mitotic index (percentage of cells in mitosis) and nodule diameter at 12, 18, and 24 days after inoculation.

observed in effective nodule formation (Newcomb 1976).

Differentiation of Infected Cells

Usually the number of rhizobia increases manyfold such that eventually the pea cytoplasm becomes densely packed with the endophyte (Figs. 9–14). The free bacteria are usually surrounded by a complete membrane when only a few bacteria are present in the host cell (Fig. 20). Later when the number of bacteria has increased, many of the rhizobia may be surrounded by a whole or partial membrane envelope or, less frequently, may completely lack a membrane envelope (Figs. 21, 22*a*–22*c*, 24*a*–24*c*); in contrast, the rhizobia in effective pea nodules are surrounded by a complete membrane envelope (Fig. 23). When the number of rhizobia increases (sometimes the infected cells degenerate before this increase) such that the host cytoplasm is densely packed with endophyte, most of the rhizobia lack any portion of a membrane envelope (Figs. 24*a*–24*c*). The host cytoplasm is present directly adjacent to the endophyte cells (Figs. 22*b* and 22*c*) so that no electron-translucent space, peribacteriodal space, surrounds the rhizobia as occurs in the infected cells of effective pea nodules (Fig. 23) (Newcomb 1976). The bacteria are pleiomorphic (Figs. 24*b* and 24*c*) but usually do not form Y-shaped bacteroids as occurs in effective pea nodules. In addition, the development of the host cell organelles in the ineffective pea nodules differs from those of effective pea nodules. In the case of ineffective pea nodules, most of the pea ribosomes are free and polyribosomes and endoplasmic reticulum are scarce (Fig. 20). Amyloplasts often assume extremely irregular configurations (Fig. 20), and large starch granules occur within them (Figs. 10–15). Many infected cells have many amyloplasts often with large irregularly shaped starch granules when the number of rhizobia is small or when rhizobia are being released from the infection thread (Figs. 8, 10–12). A single large vacuole is often present during the early stages in infected cells (Figs. 9–13); generally in later stages the vacuole is smaller or lacking, while the amount of starch is greater (Figs. 14, 15). The pea cell nucleus, which has a prominent nucleolus (Figs. 9–13), undergoes an increase in volume during the infection process and rhizobial multiplication but the increase seems to be less than that occurring in effective pea nodules. Senescence involves a degeneration of the host cytoplasm before bacterial death (Fig. 15).

Uninfected Cells

Most cells comprising the central zone of the nodule are uninfected (Fig. 7). These cells typically have a single large central vacuole, a large nucleus with a small nucleolus, and many circular or oval, regularly shaped amyloplasts containing large starch granules (Figs. 9, 12, 14, and 15).

Transfer Cells

Cells with cell wall ingrowths, transfer cells (Gunning and Pate 1969), occur in two locations in pea root nodules. Wall ingrowths are present in pericycle cells of effective (Pate *et al.* 1969) and ineffective (Fig. 25*a*) pea root nodules. Transfer cells also occur in the xylem parenchyma cells of the lateral root adjacent to both ineffective and effective pea root nodules (Newcomb and Peterson, unpublished observations). The wall ingrowths are similar in both types of pea nodule. The ingrowths are generally branched in pericycle cells (Fig. 25*b* while they are unbranched in xylem parenchyma cells; the

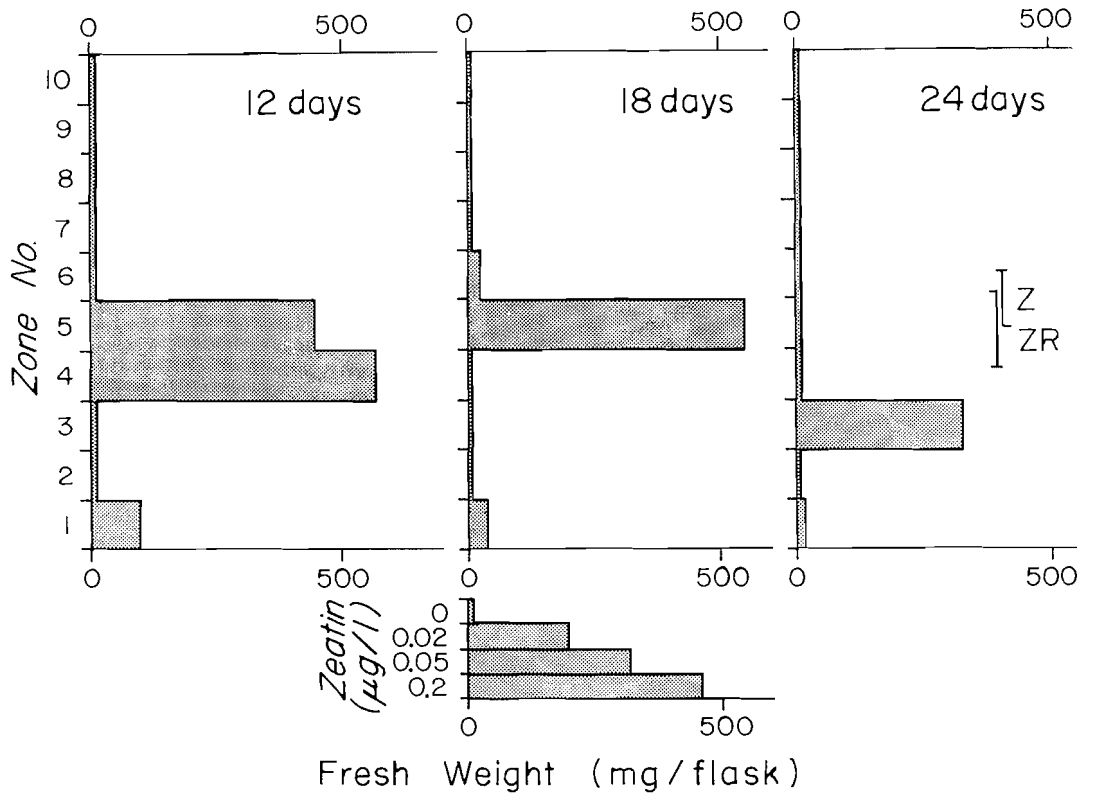

FIG. 5. Graph of the growth response of soybean callus tissue to the butanol extract after thin-layer chromatography. The R_f values for known samples of zeatin (Z) and zeatin riboside (ZR) run at the same time are indicated. Fresh-weight increases in the callus bioassay are shown for known concentrations of zeatin.

ingrowths are of similar size in both types of nodule.

Discussion

Peas of the cultivar Little Marvel infected with the ineffective strain 1019 of *R. leguminosarum* differ greatly from peas of the same cultivar infected with the effective strain 128 C53. Plants inoculated with strain 1019 are smaller than those infected with the effective strain; the fresh weight of roots and shoots as well as fruit and flower length are reduced in plants infected with the ineffective strain (cf. Fig. 1 with Fig. 1 in Syōno *et al.* 1976). In addition, less nodule mass is produced on the plant inoculated with strain 1019; fewer and smaller nodules occur on plants infected with strain 1019 as compared with those infected with 128 C53 (cf. Figs. 3 and 4 with Figs. 3, 4, and 5 in Syōno *et al.* 1976). The slower growth rate of the ineffective nodules and their smaller size may be related to the earlier cessation of mitotic activity in the ineffective pea nodules than in effective pea nodules (cf. Fig. 4 with Fig. 7 in Syōno *et al.* 1976). The decline in mitotic activity corresponds with a decline in cytokinin content in both ineffective and effective pea nodules (cf. Fig. 2 with Fig. 6 in Syōno *et al.* 1976). In effective pea nodules, cytokinins are undetectable in 5-week-old nodules that lack a nodule meristem; in earlier stages there is a progressive decline in mitotic activity and cytokinin content. Furthermore, in 3- and 4-week-old effective pea nodules much of the cytokinin is present in the region of the nodule meristem, the only site of mitosis in the nodule (Syōno *et al.* 1976). Mitotic activity of ineffective nodules declines sooner than that observed in effective nodules (cf. Fig. 4 with Fig. 7 in Syōno *et al.* 1976). Similarly, cytokinin content declines such that the con-

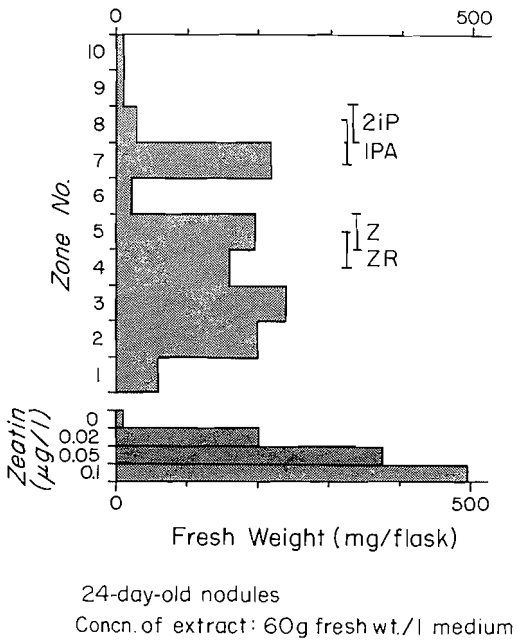

FIG. 6. Soybean callus assay of extract of 24-day-old ineffective nodules after thin-layer chromatography. See text for explanation. Concn., concentration; wt., weight.

centration is very low in 24-day-old ineffective pea nodules (Fig. 2). The smaller size of the ineffective nodules is probably due to the early decline of cytokinins and cessation of mitotic activity in the nodule meristem. In pea root nodules mitosis occurs only in the nodule meristem, which is the source of most of the cells comprising the various tissues of the nodule. Thus, a lack of mitotic activity would limit subsequent nodule growth to that associated with cell enlargement.

Qualitatively the cytokinins of ineffective pea nodules differ from those extracted from effective pea nodules since a new and unidentified cytokinin appears in 24-day-old ineffective nodules (Figs. 5 and 6). This compound has not been detected in younger ineffective pea nodules nor in effective pea nodules (Syōno and Torrey 1976). When grown alone in pure culture, *R. leguminosarum* produces IPA and two unknown cytokinins (Giannattasis and Coppopa 1969). Effective pea nodules contain two groups of cytokinins, i.e., zeatin and its immediate derivatives and 2iP and its derivatives (Syōno and Torrey 1976). However, the mechanisms and sites of cytokinin synthesis within the nodule are not known and several hypotheses regarding the symbiotic biosynthesis of these phytohormones have been suggested (Syōno and Torrey 1976). The invading rhizobia may produce 2iP and related compounds while the pea nodule meristem may be the main source of zeatin and its derivatives; both types of cytokinin could function in stimulating deoxyribonucleic acid (DNA) synthesis and mitosis of the cells of the developing nodule. Another possibility is that bacterially produced 2iP is converted to zeatin and its derivatives by the pea tissue and only zeatin functions in stimulating mitotic activity of the host cells. A third alternative is that early events of nodule morphogenesis are controlled by the bacterial cytokinin 2iP and subsequent events are controlled by zeatin synthesized by the host tissue. The occurrence of another cytokinin in the ineffective nodules produced by the mutant strain 1019 adds credibility to the idea that both bacterial and legume cytokinins are involved in controlling nodule morphogenesis. Clearly the unidentified cytokinin produced in older ineffective nodules results from the presence and activity of the ineffective bacterial strain. Cytokinin biosynthesis may well be another symbiotic activity involving the genomes and metabolic pathways of both partners.

The relationship of cytokinin content and biosynthesis to the morphological and fine structural differences observed between the ineffective and effective pea nodules is not clear. However, it appears that general synthetic activity is not stimulated as much in the infected cells of the ineffective nodules as in the effective nodules. Polyribosomes and endoplasmic reticulum are scarce in the infected cells of ineffective pea nodules; such is not the case in effective pea nodules (Newcomb 1976). The general scarcity of endoplasmic reticulum and later the lack of complete membrane envelopes surrounding the free rhizobia in the ineffective nodules may reflect an alteration of membrane biosynthesis. While a few rhizobia emerging from the unwalled droplets of the infection thread lack complete membrane envelopes, usually the absence of a complete membrane envelope occurs after the number of free rhizobia has increased manyfold in the host cytoplasm.

The occurrence of transfer cells in an ineffective nodule is reported for the first time. Pate *et al.* (1969) reported the absence of pericyle transfer cells in several species, although it was not clear if any of these species had transfer

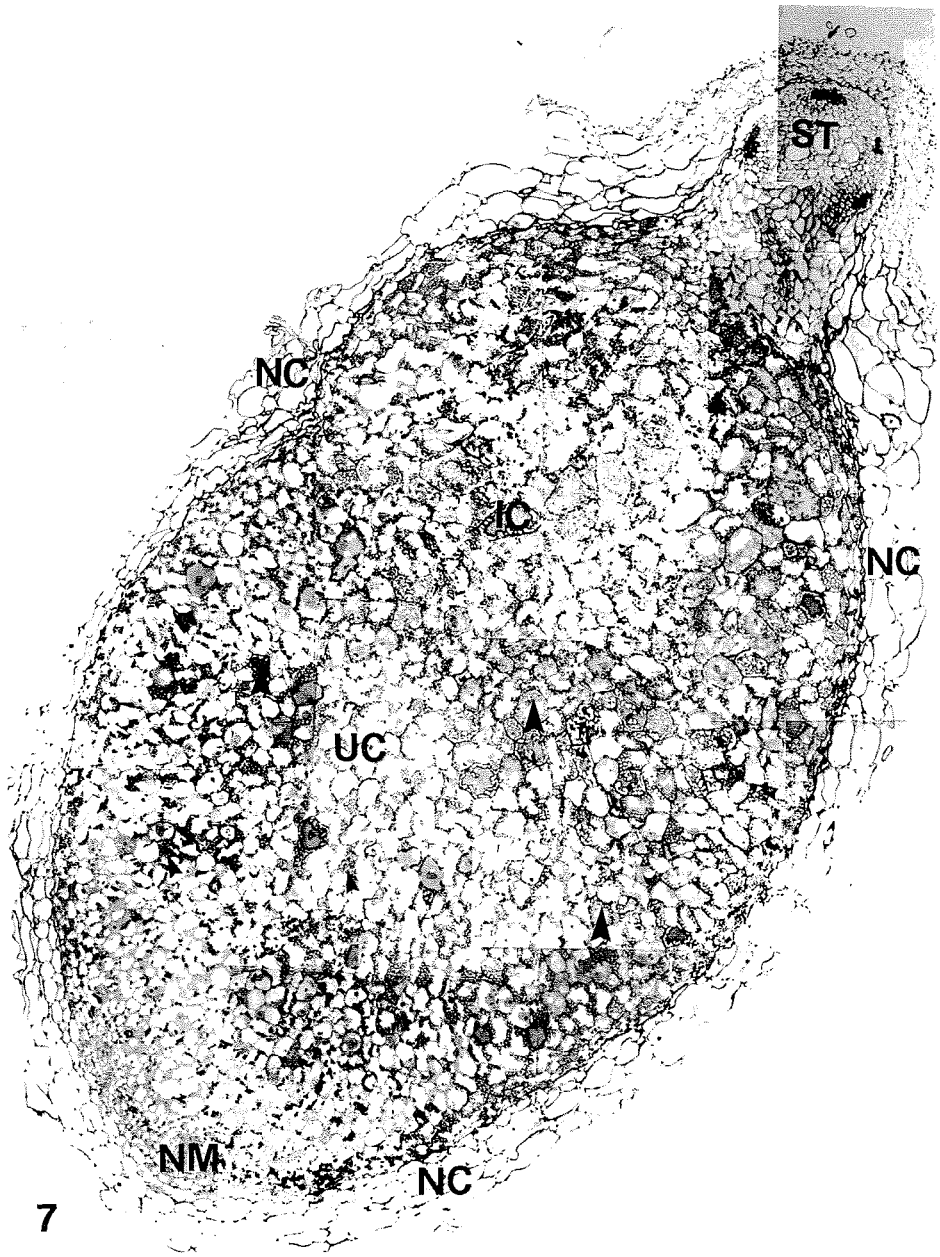

FIG. 7. Light microscopic montage of a longitudinal section of a 15-day-old ineffective pea nodule. Shown are the nodule cortex (NC), the nodule meristem (NM), the central zone of infected (IC) and uninfected (UC) cells, and the stele (ST) of the lateral root. Note the numerous amyloplasts with large starch granules (arrows) in the cells of the central zone and the random arrangement of cells in this zone as contrasted with the orderly developmental sequence found in effective pea nodules (cf. Fig. 1 Newcomb (1976) and Fig. 1 Syōno *et al.* (1976)). × 74.

cells in effective nodules. Wall ingrowth formation generally coincides with the start of solute transport (Pate and Gunning 1972). Since ineffective nodules do not fix molecular nitrogen, the export from the nodule of amino acids is probably not the stimulus for wall ingrowth formation.

In effective nodules of pea, each bacteroid has

a complete membrane of host origin surrounding it (Newcomb 1976). In rare cases two bacteria occur within a single membrane. This relationship suggests that in the effective nodule, bacteria once released seldom divide again. In the ineffective nodules where host membranes

FIG. 8. Light micrograph illustrating a cell being invaded by an infection thread (IT) with unwalled droplets (large arrow) from which rhizobia (small arrows) are being released into the pea cytoplasm. Numerous round amyloplasts (A) are located at the periphery of this cell which also contains a large vacuole (V). The cell at the left of the figure contains a few free rhizobia (small arrows) and many large irregularly shaped amyloplasts (A). × 940. FIG. 9. Light micrograph of a cell being invaded by an infection thread (IT) with an unwalled droplet (large arrow) containing a few rhizobia (small arrows) and an enlarged nucleus with a large vacuolate nucleolus (Nu). Also shown are two uninfected cells (*) with numerous round amyloplasts (A). × 900. FIG. 10. Light micrograph of a cell containing many amyloplasts (A) with large irregularly shaped starch granules. Rhizobia (small arrows) are being released from the unwalled portion of the infection thread (IT). Also shown are the host pea nucleus (N), which possesses a prominent nucleolus, and adjacent uninfected cells (*). × 940. FIG. 11. Light micrograph of an infected cell having a few rhizobia (arrows), a large nucleus (N) with a prominent nucleolus, an unwalled droplet (UD), large vacuoles (V), and many regularly shaped amyloplasts (A). Note the dense concentration of amyloplasts in the adjacent cell. × 960. FIG. 12. Light micrograph of a young infected cell possessing a small number of free rhizobia (arrows), a large nucleus (N) and nucleolus, many small amyloplasts (A), and large vacuoles (V). Also shown is an adjacent infected cell that contains more free rhizobia (arrows) and larger amyloplasts. A portion of an uninfected cell (*) with many amyloplasts is seen at the lower right. × 950. FIG. 13. Light micrograph of a young infected cell that contains more free rhizobia (small arrows) than cells shown in Figs. 8 and 10–12 but contains only a few small amyloplasts (large arrow). Numerous adjacent vacuolate uninfected cells are also shown. × 880. FIG. 14. Light micrograph of two infected cells containing large numbers of rhizobia (arrows) and numerous amyloplasts (A). Adjacent uninfected cells (*) are also seen. × 830. FIG. 15. Light micrograph of a senescing infected cell and adjacent nonsenescing uninfected cells (*), one of which contains an infection thread (IT). Note that the amyloplasts in the uninfected cells are more regularly shaped than those present in the infected cells. × 840.

FIG. 16. Electron micrograph of a portion of an unwalled droplet from which rhizobia (R) are being released into the pea cytoplasm. The pea plasma membrane (arrows) bounds the thread matrix (TM) of the unwalled droplet and almost completely surrounds the escaping rhizobium. × 31 200. FIG. 17. Electron micrograph of a rhizobium (R) escaping from an unwalled droplet. The plasma membrane (arrows) separates the thread matrix (TM) from the host cytoplasm and surrounds the escaping rhizobium. Note the dense appearance of the rhizobium. × 39 770. FIG. 18. Electron micrograph showing two rhizobia located near an unwalled droplet. The free rhizobium is partially surrounded by a membrane envelope (arrows) while the escaping bacterium is almost completely surrounded by the host plasma membrane (arrows), which is continuous with the portion separating the thread matrix (TM) from the host cytoplasm. Note the dense appearance of the bacterium which may be senescent. × 32 670. FIG. 19. Electron micrograph of the terminal portion of an infection thread which is bounded by pea cell wall (CW) and a plasma membrane (arrows) that eventually forms membrane envelopes (double arrows) around the escaping rhizobia (R). Compare the healthy appearance of the rhizobia with those shown in Figs. 17 and 18. × 28 300.

FIG. 20. Electron micrograph of a portion of an infected cell that contains only a few free rhizobia. Shown are a single rhizobium (R) surrounded by a membrane envelope (arrows), two irregularly shaped amyloplasts (A) with small starch granules (S), numerous mitochondria (M), and a portion of the nucleus (N). Most of the ribosomes are free as polyribosomes and endoplasmic reticula are generally scarce in infected cells of ineffective pea nodules. × 16 720. FIG. 21. Electron micrograph of an infected cell containing numerous rhizobia that are surrounded by partial membrane envelopes (large arrows). Also shown are Golgi bodies (G), a proplastid (P), a large mitochondrion (M), and a few polyribosomes (small arrows). × 19 820.

FIG. 22*a*. Electron micrograph of a vacuolate infected cell that contains numerous rhizobia with and without membrane envelopes. The letters *b* and *c* indicate portions which are shown in Figs. 22*b* and 22*c*. × 1390. FIG. 22*b*. Higher magnification of area *b* in Fig. 22*a*. Shown are an amyloplast (A) with a single starch granule (S), several proplastids (P) and mitochondria (M), and numerous rhizobia (R). The rhizobia are bounded by a partial membrane envelope (arrows) and most lack a peribacteroidal space (*). × 20 480. FIG. 22*c*. Higher magnification of area *c* in Fig. 22*a*. Shown are a mitochondrion (M), profiles of rough endoplasmic reticulum (RER), and five rhizobia. Four of the rhizobia lack peribacteroidal spaces and appear to be bounded by only small pieces of membrane envelope (arrows). The remaining rhizobium appears to have a complete membrane envelope (arrows) but has an abnormal peribacteroidal space (*); cf. Fig. 23. × 26 890. FIG. 23. Electron micrograph of an infected cell from a 2-week-old effective pea root nodule (cf. Newcomb 1976). The rhizobia (R) are surrounded by a peribacteroidal space (PBS) which is bounded by a complete membrane envelope (arrows). × 9600.

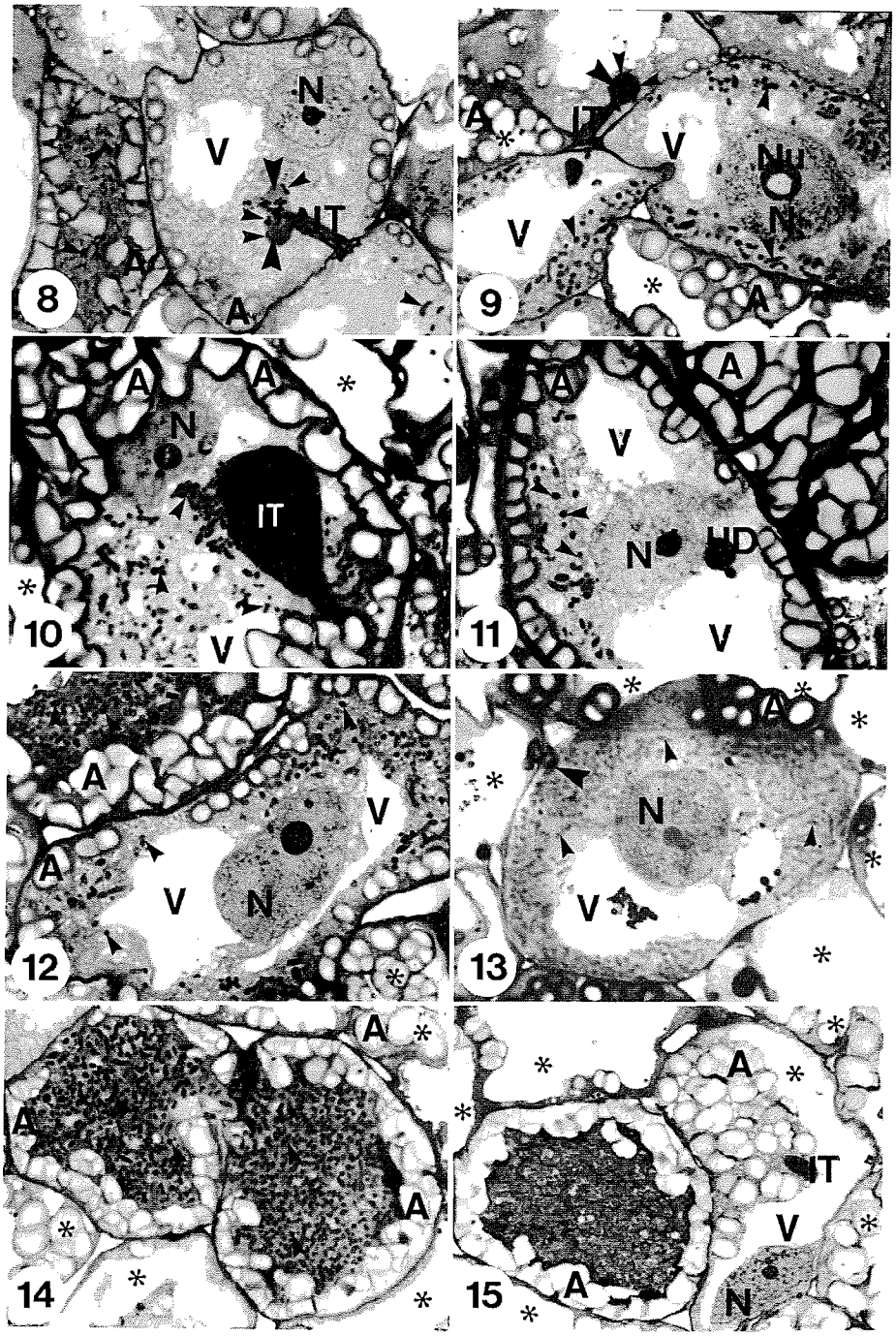

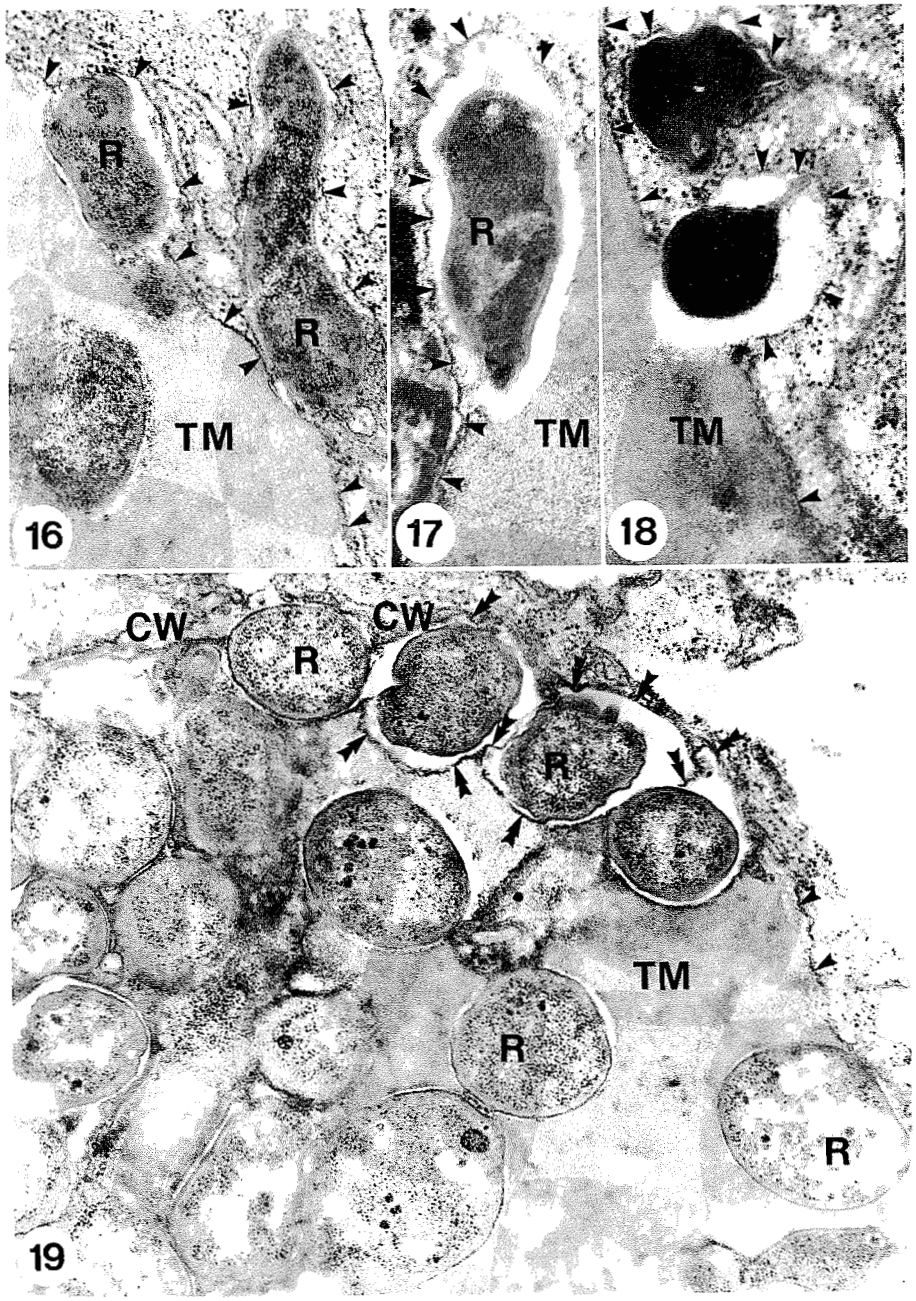

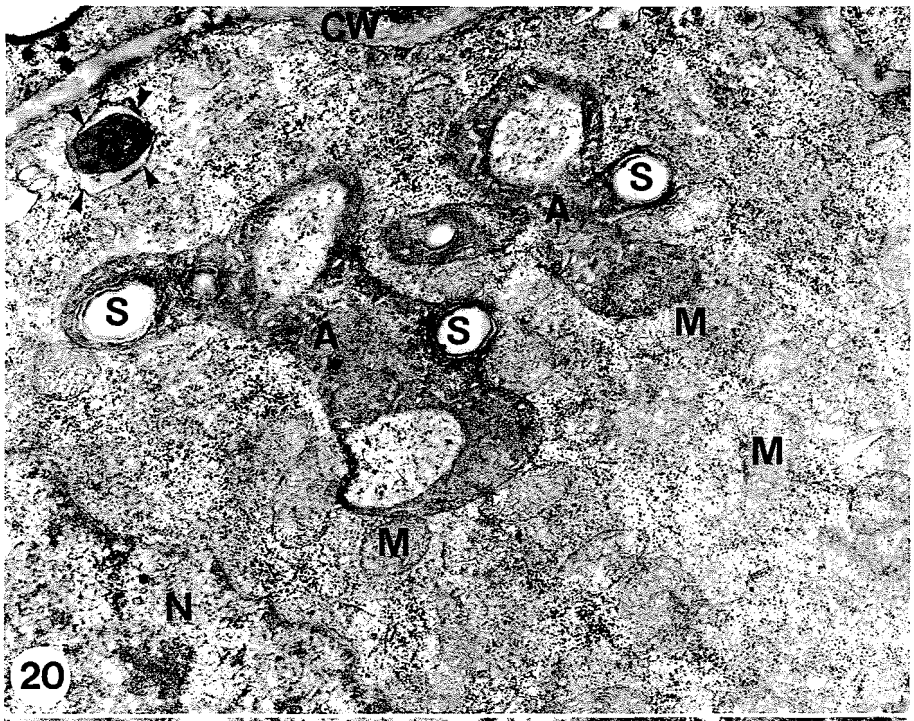

20

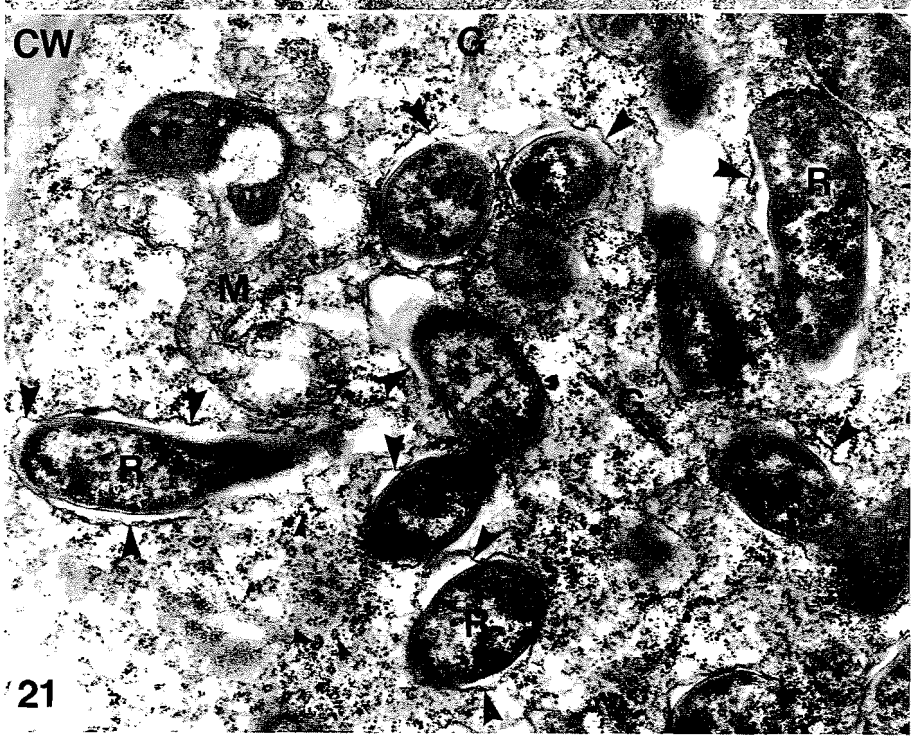

21

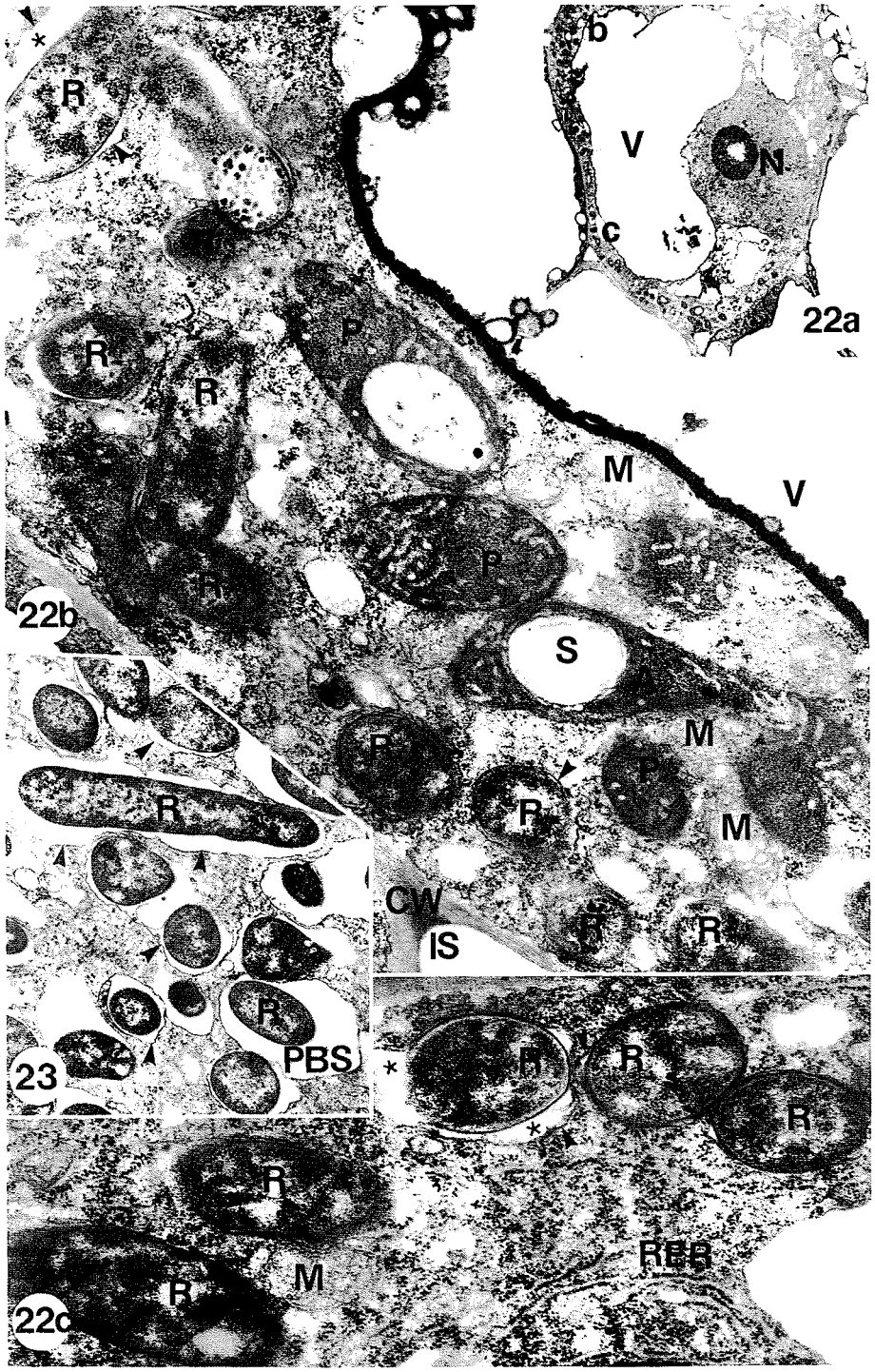

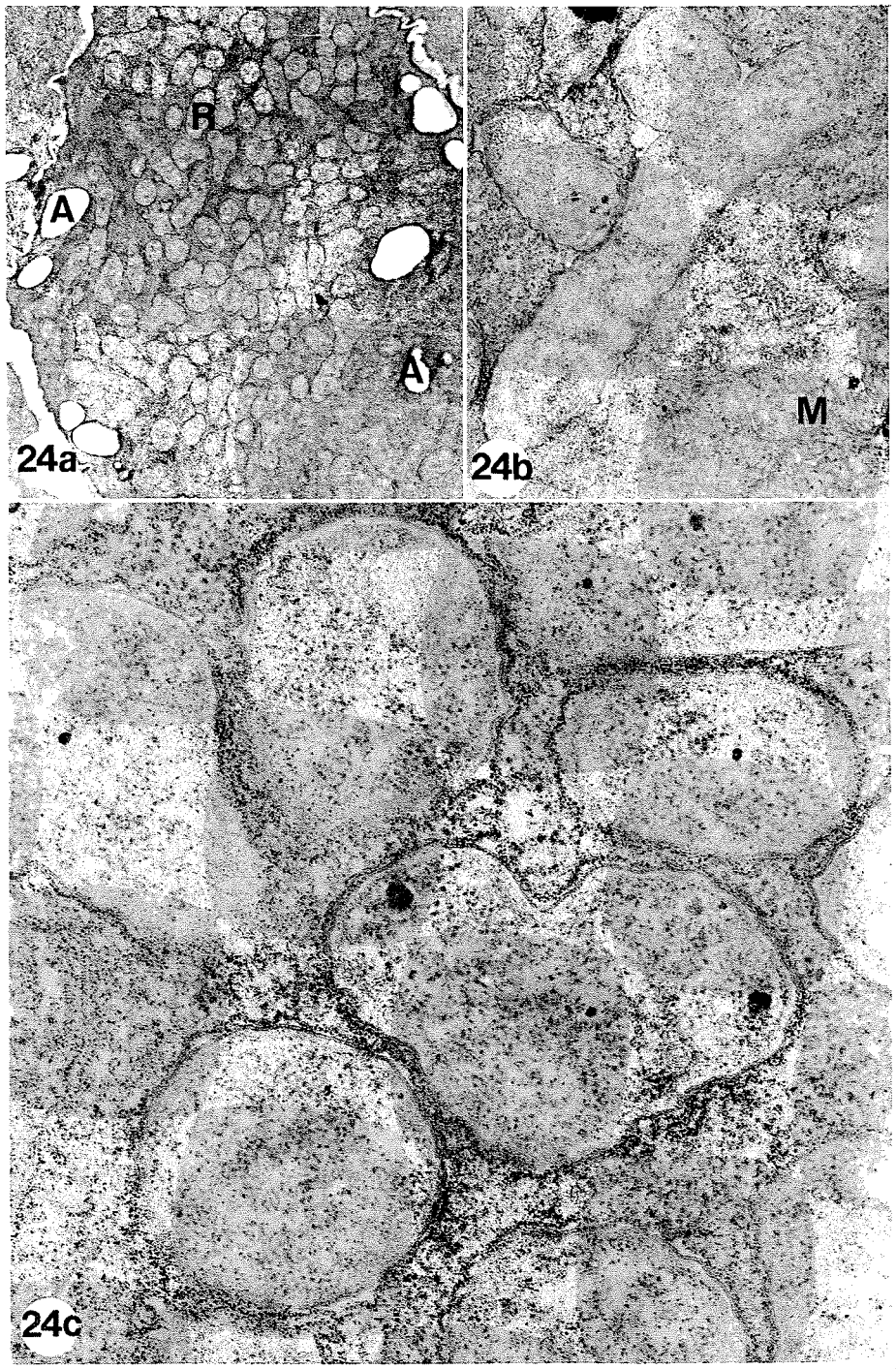

FIG. 24*a*. Electron micrograph of an infected cell containing many free rhizobia (R), none of which are surrounded by a complete membrane envelope (arrows). Amyloplasts (A) are also present. × 5450. FIG. 24*b*. Higher magnification of a branched rhizobium shown in Fig. 24*a*. No membrane envelope is associated with this bacterium. × 23 080. FIG. 24*c*. Higher magnification of rhizobia in the infected cell illustrated in Fig. 24*a*. Note the absence of complete membrane envelopes surrounding the rhizobia. × 60 670.

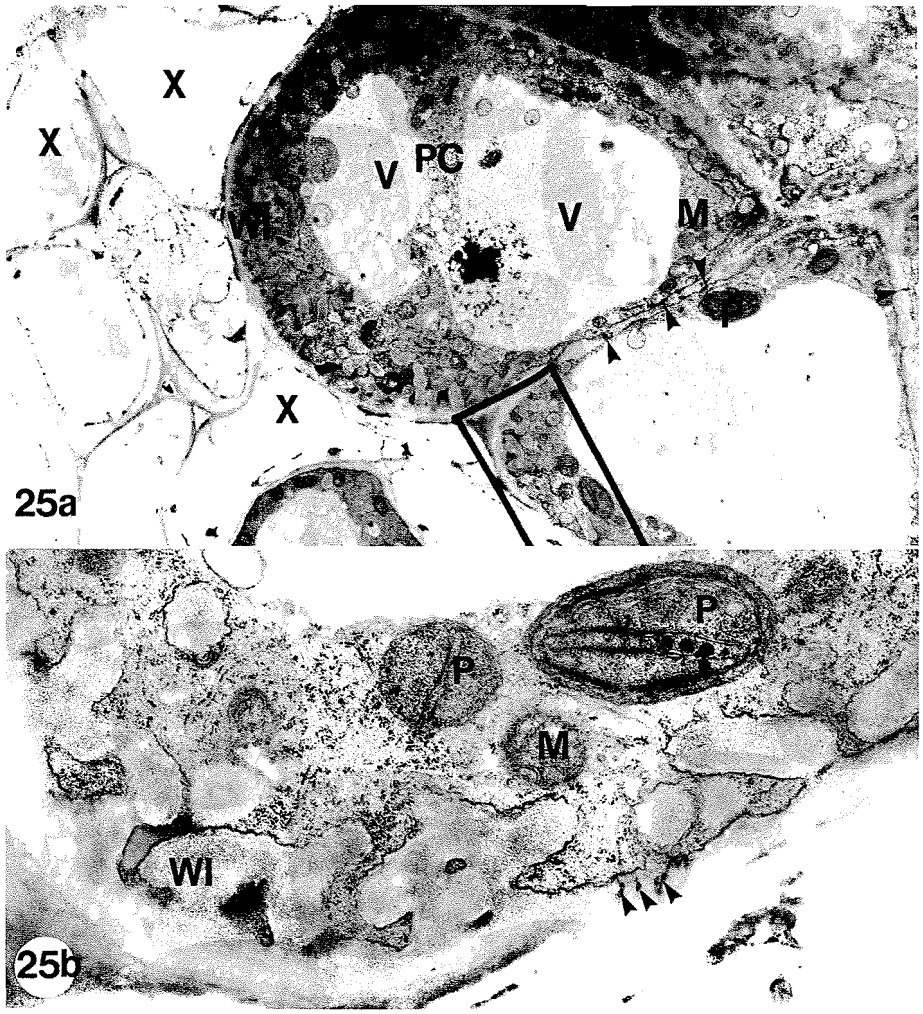

FIG. 25*a*. Electron micrograph of xylem (X) and pericycle cells (PC) in the lateral root tissue adjacent to an ineffective pea root nodule. Wall ingrowths (WI) are present in the pericycle cells on the regions of cell wall adjacent to xylem. Proplastids (P), numerous mitochondria (M), plasmodesmata (arrows), and large vacuoles are also present in the pericycle. × 3670. FIG. 25*b*. Higher magnification of the outlined area in Fig. 25*a*. The wall ingrowths are branched and plasmodesmata (arrows) occur in the wall on which the wall growths develop. × 19 340.

are not rigorously formed about each bacterium upon its release, many bacteria are found free in the host cytoplasm, presumably free to multiply and (or) disrupt the biosynthetic machinery of the host cells. The enzyme nitrogenase is associated with bacteroids in effective nodules. It is believed that the host membranes surrounding the bacteria provide the protected environment for development of the enzyme within it. In this case, the ineffective bacterial strain fails to establish a true bacteroid structure owing to lack of membrane formation and the enzyme is not formed. It is not known if there is a connection between the altered quantitative and qualitative aspects of cytokinin synthesis and the reduced levels of cytoplasmic membranes. The absence of leghaemoglobin occurs frequently in ineffective nodules (Bergersen 1957; Chandler *et al.* 1974; Dart 1975), but the disputed location of this compound (Burns and Hardy 1975) makes it difficult to relate this alteration to the absence of the membrane envelope. The development of a green pigmentation in the senescing nodules is at present unexplained. At no time were chloroplasts observed during the ultrastructural studies of the

nodules. Possibly the green color is related to oxidized products of haemoglobin but not formed in the usual way. Similar green pigmentation in ineffective nodules has been reported earlier (Maier and Brill 1976). Clearly neither alternation is beneficial for an effective symbiosis. The abundance of large starch granules in the amyloplasts of ineffective pea nodules and the accelerated degeneration of infected cells agree with previous observations on other ineffective legume nodules (Bergersen 1957; Schwinghamer 1964; Chandler *et al.* 1974: Dart 1974, 1975). However, the absence of a membrane envelope surrounding the endophyte when the bacterial population reaches its maximum in the infected cells seems to be unique for ineffective pea nodules infected with strain 1019 of *R. leguminosarum*.

Acknowledgments

The authors are indebted to Mrs. Shirley LaPointe and Mr. Peter Del Tredici for growing the plants, Mr. Dale Callaham for embedding the tissues in plastic, Ms. Patricia Goforth for culturing the *Rhizobium*, and Dr. R. L. Peterson for his constructive criticisms. K. Syōno and W. Newcomb are grateful for being recipients of Maria Moors Cabot Postdoctoral Research Fellowships when this study was initiated. The authors also appreciate being able to use the electron microscopes of Drs. B. Lu and Otto Stein at the Universities of Guelph and Massachusetts, respectively. We are indebted to the Microbiology Department of the Rothamsted Experiment Station, Harpenden, Herts., England, for providing us with a culture of *Rhizobium leguminosarum* strain 1019 used in these studies. The research was supported by the Maria Moors Cabot Foundation for Botanical Research of Harvard University, Research grant BMS-74-20563 of the United States of America National Science Foundation, and an operating grant from the National Research Council of Canada to Dr. R. L. Peterson.

BERGERSEN, F. J. 1957. The structure of ineffective root nodules of legumes: an unusual new type of ineffectiveness, and an appraisal of present knowledge. Aust. J. Biol. Sci. **10**: 233–242.

——— 1974. Formation and function of bacteroids. *In* The biology of nitrogen fixation. *Edited by* A. Quispel. North Holland Publishing Co., Amsterdam. pp. 473–498.

BRILL, W. J. 1974. Genetics of N_2-fixing organisms. *In* The biology of nitrogen fixation. *Edited by* A. Quispel. North Holland Publishing Co., Amsterdam. pp. 639–660.

BURNS, R. C., and R. W. F. HARDY. 1975. Nitrogen fixation in bacteria and higher plants. Springer-Verlag, New York.

CHANDLER, M., P. J. DART, and P. S. NUTMAN. 1974. The fine structure of hereditary ineffective red clover nodules. Rothamsted Exp. Stn. Rep. 1973, Part 1, Harpenden, Herts., England. pp. 83–84.

DART, P. J. 1974. The infection process. *In* The biology of nitrogen fixation. *Edited by* A. Quispel. North Holland Publishing Co. Amsterdam. pp. 381–429.

——— 1975. Legume root nodule initiation and development. *In* The development and function of roots. *Edited by* J. G. Torrey and D. T. Clarkson. Academic Press, London. pp. 467–506.

GIANNATTASIS, M., and S. COPPOPA. 1969. Isolamento di citochinine dal *Rhizobium leguminosarum* Frank. Giorn. Bot. Ital. **103**: 11–17.

GUNNING, B. E. S., and J. S. PATE. 1969. "Transfer cells," plant cells with wall ingrowths, specialized in relation to short distance transport of solutes—their occurrence, structure and development. Protoplasma, **68**: 107–133.

HOLL, F. B. 1973. A nodulating strain of *Pisum* unable to fix nitrogen. Plant Physiol. (Suppl.), **51**: 35.

——— 1975. Host plant control of the inheritance of dinitrogen fixation in the *Pisum–Rhizobium* symbiosis. Euphytica, **24**: 767–770.

MAIER, R. J., and W. J. BRILL. 1976. Ineffective and nonnodulating mutant strains of *Rhizobium japonicum*. J. Bacteriol. **127**: 763–769.

NEWCOMB, W. 1976. A correlated light and electron microscopic study of symbiotic growth and differentiation in *Pisum sativum* root nodules. Can. J. Bot. **54**: 2163–2186.

NUTMAN, P. S. 1969. Genetics of symbiosis and nitrogen fixation in legumes. Proc. R. Soc. London, Ser. B, **172**: 417–437.

PANKHURST, C. E. 1974. Ineffective *Rhizobium trifolii* mutants examined by immune-diffusion, gel-electrophoresis, and electron microscopy. J. Gen. Microbiol. **82**: 405–413.

PATE, J. S., and B. E. S. GUNNING. 1972. Transfer cells. *In* Annual review of plant physiology. *Edited by* L. Machlis. Annual Reviews Inc., Palo Alto, CA. pp. 173–196.

PATE, J. S., B. E. S. GUNNING, and L. G. BRIARTY. 1969. Ultrastructure and functioning of the transport system of the leguminous root nodule. Planta (Berlin), **85**: 11–34.

SCHWINGHAMER, E. A. 1964. Association between antibiotic resistance and ineffectiveness in mutant strains of *Rhizobium* spp. Can. J. Microbiol. **10**: 221–233.

SYŌNO, K., W. NEWCOMB, and J. G. TORREY. 1976. Cytokinin production in relation to the development of pea root nodules. Can. J. Bot. **54**: 2155–2162.

SYŌNO, K., and J. G. TORREY. 1976. Identification of cytokinins in root nodules of the garden pea, *Pisum sativum* L. Plant Physiol. **57**: 602–606.

VENABLE, J. H., and R. COGGESHALL. 1965. A simplified lead citrate stain for use in electron microscopy. J. Cell Biol. **25**: 407–408.

ZOBEL, R. W., P. DEL TREDICI, and J. G. TORREY. 1976. A method for growing plants aeroponically. Plant Physiol. **57**: 344–346.